Catena 87 (2011) 119–128

Contents lists available at ScienceDirect

Catena

journal homepage: www.elsevier.com/locate/catena

Impact of rainfall and topography on the distribution of clays and major cations in granitic catenas of southern Africa

Lesego Khomo [a,*], Anthony S. Hartshorn [b], Kevin H. Rogers [c], Oliver A. Chadwick [d]

[a] Max-Planck-Institut für Biogeochemie, 10 Hans-Knöll-Str. 07745, Jena, Germany
[b] Department of Geology and Environmental Science, James Madison University, Harrisonburg, VA 22807, USA
[c] Centre for Water in the Environment, School of Animal, Plants, and Environmental Sciences, Witwatersrand University, Johannesburg, PO Wits 2050, South Africa
[d] Department of Geography, University of California, Santa Barbara, CA 93106-4060, USA

A R T I C L E I N F O

Article history:
Received 26 April 2010
Received in revised form 2 May 2011
Accepted 18 May 2011

Keywords:
Soil
Arid/semi-arid/sub-humid rainfall
Soil development
Clay mineralogy
Kruger National Park

A B S T R A C T

Soil catenas integrate and amplify gravity transfer and differentiation processes of eluviation and illuviation in soil profiles. We quantified differences in these redistribution processes along granitic catenas across an arid to sub-humid climate gradient in Kruger National Park, South Africa. We measured soil properties in nine catenas sampled from three areas receiving annual rainfall of 470 mm (arid zone), 550 mm (semi-arid zone) and 730 mm (sub-humid zone). As rainfall increased, kaolinite replaced smectite as the dominant clay mineral in all landscape positions across the catenas. Toeslopes showed the strongest evidence of this transition with an excess of smectite in the arid catenas but complete prevalence of kaolinite in toeslopes of sub-humid catenas. The concentration and distribution of clay along the catenas were dependent on landscape position as well — soil profiles at and near the crests were clay depleted (as low as 1%) while those at the toeslopes had much more clay (up to 60%). Clay redistribution along catenas was sensitive to climate with the least amount of redistribution occurring in the dry sites and the most occurring in the wet sites. As a consequence, the sub-humid catenas had clay accumulation only in a small part of the toeslopes while the bulk of their length was represented by highly leached soils. In contrast, arid zone catenas showed little clay redistribution and semi-arid sites displayed the greatest within-catena clay redistribution and preservation. Clay movement and storage conditioned other soil properties such as CEC, base cation distribution, base saturation and pH.

1. Introduction

Catenas are hydrologically linked hillslope soils first described by Milne (1935) in east Africa. Subsequent work has demonstrated that the catena concept has broad geographic applicability as a framework for understanding soils (Nye, 1954; Radwanski and Ollier, 1959; Watson, 1964) and ecosystems (Dye and Walker, 1980; Scholes and Walker, 1993; Venter et al., 2003) in Africa particularly but generally in all stable continental interiors (Paton et al., 1995). Central to catena formation is the upslope mobilization, downslope redistribution and transfer of solutes, colloids and particles culminating in soil differentiation across hillslopes (Conacher and Dalrymple, 1977; Huggett, 1975). Differences in mobilization characteristics, transport pathways and total water flux lead to different degrees of differentiation and soil properties along catenas much like they do in individual soil profiles (Birkeland, 1999; Sommer et al., 2000). Therefore, in theory, catenas can be classified based on their chemical and morphological heterogeneity between crests and valleys as they respond to soil forming factors such as rainfall, geology and topography (Sommer and Schlichting, 1997). In practice, there are few explicit studies that explore the impact of climate on catena properties where other soil-forming factors such as geology are constrained.

Here, we investigate granitic catenas where clays and solutes are mobilized and redistributed to differing extents depending primarily on climate and secondarily on slope-length. As with vertical redistribution of clays and ions within soil profiles these properties are highly sensitive to effective moisture (Chadwick and Graham, 1999; Chadwick et al., 2003). We sampled soils along catenas receiving 470 mm (arid), 550 mm (semi-arid) and 730 mm (sub-humid) of rain annually, and determined differences in the downslope distribution of soil pH, concentration of exchangeable base cations, concentration of clays and their mineralogy. Three catenas representing different slope-length were sampled in each rainfall zone to provide an understanding of differences in catena properties associated with variation in slope gradient and local relief.

We had previously sampled soils on hillcrests in the three rainfall zones and found that all crest soils had lost major elements relative to

* Corresponding author.
E-mail address: lesegok@gmail.com (L. Khomo).

0341-8162/$ – see front matter © 2011 Elsevier B.V. All rights reserved.
doi:10.1016/j.catena.2011.05.017

parent material, and base cation saturations declined from 80 to 35% with rising rainfall (Khomo, 2008). While kaolinite was found at all sites, smectite was identified only in the crest soils of the driest site. We also found an increase in total clay content in the crests from 30 ± 16 kg m^{-2} in the arid zone (n = 4), to 42 ± 16 kg m^{-2} in the semi-arid zone (n = 5), and 306 ± 132 kg m^{-2} in the sub-humid zone (n = 4). In aggregate, the crest sites suggest that even though annual rainfall is fairly low across Kruger National Park, the soils become strongly leached as rainfall increases, which leads to significant changes in soil properties across the gradient. It therefore appears that these crest soils are an important source of ions and clays that can augment soil constituent accumulation downslope. Here we evaluate the role of rainfall and topography in driving variations in mobilization, redistribution and accumulation of soil constituents. For the first time as far as we know, multiple catenas were utilized quantitatively to explore how catena soil properties vary spatially as mediated by varying inputs of rainfall. Therefore, these data will provide useful context material for future pedo-geomorphic studies in the region and elsewhere.

2. Field sites, materials and methods

The ~2 million ha Kruger National Park is located in the northeast corner of South Africa along the border with Mozambique where there is relatively little impact of human land use (Fig. 1). Our field sites were located in the western half of the park which is mostly underlain by granitoid rocks associated with the >3 Ga Kaapval Craton and forms a low-gradient landscape bounded by Karoo volcanics in the east and the Great Escarpment to the west (Barton et al., 1986). The characteristic vegetation of the region is bush savanna, with broad- and fine-leafed vegetation in clay-poor and clay-rich soils, respectively. This soil-vegetation association is observed on granitic parent material throughout the park (Gertenbach, 1983) and in other parts of southern Africa (Scholes and Walker, 1993).

We sampled 62 pedons to rock or saprolite on 9 catenas across a 250 km transect extending from a mean annual precipitation (MAP) of 470 mm in the north (arid zone Shingwedzi) to 730 mm in the southwest of the park (sub-humid Pretoriuskop) while the intermediate rainfall zone had 550 mm MAP (semi-arid Skukuza). Mean annual air temperatures ranged from 24 °C in the arid zone to 22 °C in semi-arid Skukuza and 21 °C in the sub-humid catenas (Scholes et al., 2003). In each climate zone, three catenas were selected: a short catena with a steep slope (H: high) in the upper reaches of a drainage network; a mid-length catena with a gentler slope (M: middle) and a low relief and long catena in the lower reaches of the river system (L: low). Thus nine catenas were sampled across a nested matrix of rainfall and slope-length: DH, DM, DL, IH, IM, IL, WH, WM, and WL. WL was actually shorter than WM but had a gentler slope (Fig. 2) and is referred to as longer than WM for convenience, this is consistent with the relief gradient of catenas within climate zones. Fig. 2 shows catena cross sectional profiles, highlighting ranges in elevation, slope-length and slope-angle. The arid-zone catenas occurred between 300 and 365 m above mean sea level (amsl) while the sub-humid catenas were at 510–580 m amsl. The semi-arid catenas were situated between 250 and 350 m amsl. For the most part, sub-humid catenas were longer, ranging between 900 and 1376 m while arid catenas were 320 to 970 m long. Longer catenas generally had gentler slope angles, IL in Skukuza was the longest (1600 m) and the gentlest (1.1°) catena in the study. The range in depths to saprolite for the 62 pedons studied was 19 to 245 cm with minimum depths in the arid zone (64 ± 8 cm) and maximum depths in the sub-humid zone (148 ± 9 cm) while depths in the semi-arid zone were 82 ± 7 cm (Table 1).

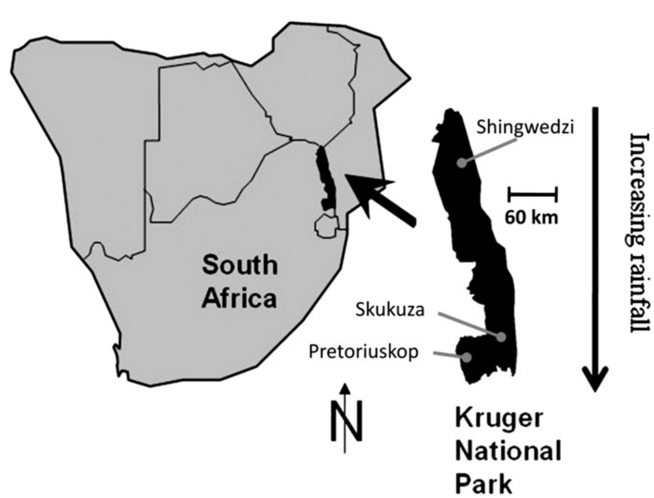

Fig. 1. Study site showing Kruger National Park, Shingwedzi in the arid north, Skukuza with intermediate/semi-arid rainfall and sub-humid Pretoriuskop.

Soil profile sampling locations (Table 1) were selected after recording changes in vegetation, surface soil color, slope breaks and morphological observations in test pits. Soil pits were excavated near the observed transitions and described and sampled using standard methods (Schoeneberger et al., 1998) and classified according to U.S. Soil Taxonomy (USDA-NRCS, 1996). Clay in the fine-earth fraction (<2 mm) was measured by the hydrometer method following dispersal of peds with sodium metahexaphosphate (Carter, 1993). We calculated a clay contrast index (CCI) at the pedon (within-profile CCI) and catena (between-profile CCI) scales as

$$CCI = 1 - \frac{clay_{upper}}{clay_{max}} \quad (1)$$

(modified from Young, 1976). For within-profile CCI $clay_{upper}$ was the percent clay in the topmost horizon and $clay_{max}$ was the maximum clay percent in the profile. For between-profile CCI, $clay_{upper}$ was taken as the depth-weighted average clay percent at the crest and $clay_{max}$ was the highest depth-weighted clay percent across the entire catena. High CCI values indicate large differences in texture for both soil profiles and catenas. Duplex soils have a high CCI because they always have a sandy A-horizon and a sub-surface Bt horizon with substantially higher clay concentration (Fey, 2010).

Clay mineralogy was determined in B-horizons from representative soil profiles; three from DH, three from DM, three from DL, three from IH, two from IM, four from IL, two from WH and six from WL. The soils were dispersed with sodium metahexaphosphate before separating the clay from bulk soil by sedimentation (Soil Survey Staff, 1996). For each clay sample, K and Mg saturated slides were prepared and submitted for 2 h to 500 °C heat treatment and glycerol solvation respectively. The clays were mounted onto glass slides for X-ray diffraction (XRD) on a Scintag PAD-V Diffractometer (Department of Chemistry and Biochemistry, University of California, Santa Barbara) between 2 and 35° 2θ CuKα configured at: 45 kV, 35 mA, a step size of 0.05, and a dwell time of 0.5 s. Peak intensity ratios of the resulting XRD scans were then used to derive semi-quantitative abundances of clay minerals for which we only present kaolinite, smectite and quartz.

Exchangeable base cations (Ca, Mg, Na and K) and the maximum potential cation exchange capacity (CEC), buffered at pH 7, were extracted with 1 M NH_4OAC and 1 N KCl followed by 1 M NH_4OAC, respectively, and measured with atomic absorption spectrometry (the base cations) and a Lachat autoanalyzer (CEC) (Liao, 2001). Electrical conductivity (EC) and pH were measured in a 1:1 soil–water mixture after five 1-minute intervals of shaking and settling. Base saturation (BS) was calculated using the sum of bases and potential CEC.

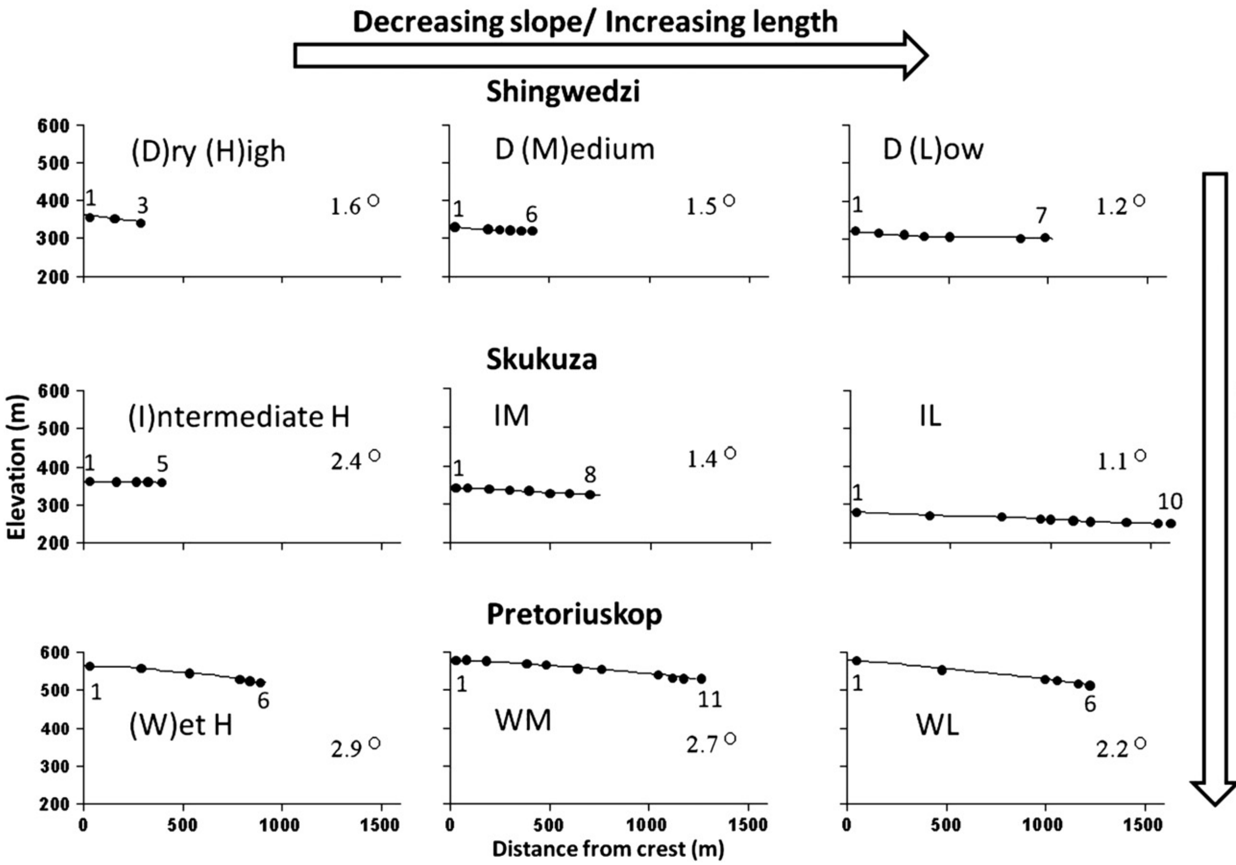

Fig. 2. Cross sections of study catenas and layout of soil profiles (black dots) between crests and toeslopes on increasingly long and gentle (slope angles shown in degrees) catenas across the arid to sub-humid rainfall gradient in Kruger National Park.

For the most part free calcium carbonate was not observed in the field, and thus we did not measure $CaCO_3$ in the lab. However, the base saturations of some toeslope horizons in the arid zone were more than 100% and often coincided with high pH, high EC and 10% 0.5 M HCl-field-effervescence (Table 2). In those cases, we interpret the excess cation concentration (>100% of CEC) to represent free salts such as carbonates dissolved during the NH_4OAC extractions, but not excessively since the pH was buffered at 7.

3. Results

3.1. Clay distribution

Between-profile clay contrast index exceeded 0.7 in seven out of the nine catenas indicating a sharp boundary separating low- and high-clay zones along the catenas (Table 3). Within-profile CCI's confirmed this dichotomy and further revealed two categories of soil texture each with a characteristic pattern in clay concentration by depth. One group had CCI>0.5 with sharp particle-size discontinuities between low-clay surface and high-clay sub-surface horizons. These soils had a duplex morphology imparted by coarse-grained surface horizons overlying clay-rich horizons formed by clay illuviation. The second group consisted of soils with CCI<0.5 indicating relatively uniform clay concentration with depth. This group was also characterized by relatively low clay concentrations (Table 3). Thus duplex soils generally occurred near the toeslopes while soils with more uniform clay concentration by depth were located in the near-crest positions. The exceptions, such as high CCI in crest and near-crest positions and low CCI in footslope soils, were due to local conditions like relatively high clay content deep within a predominantly sandy soil as in WL3 or physical erosion of the sandy topsoil in a footslope soil such that the entire profile became clay-rich resulting in low CCI as in DM5.

All catenas except DH had clay-poor upslope zones and clay-rich downslope zones schematically separated by vertical lines in Fig. 3. The vertical lines mark the point where both clay content and within-profile CCI increased in association with a shift to duplex soil morphology (Table 3) and the emergence of a seepline, the point or zone on the catena where water is diverted from sub-surface to surface flow by a downslope clay aquitard. The sequence of soil taxa between crests and footslopes of catenas was distinct from one rainfall zone to the next. In the 470 mm zone there was a switch from Haplocambids to either Paleargids or Natragids, while in the 550 mm zone soils changed from Ustorthents or Dystrustepts to Kandhaplustalfs or Natrustalfs and finally in the 730 mm zone patterns were identical to those at 550 mm except there, natric horizons were not observed. The increased rainfall from the arid/semi-arid soils between 470 and 550 mm to the sub-humid soils at 730 mm was also associated with a downslope shift in the clay-boundary leading to narrow clay-rich zones at the higher rainfall (Fig. 3). Catenas in the intermediate rainfall zone had the most extensive clay-rich zones relative to the wetter and drier catenas implying that clay storage, the balance between clay formed and clay lost, declined with both higher and lower rainfall. Intermediate upslope contributing area as indexed by slope-length was also associated with the greatest clay retention. Thus IM had maximum clay retention of all catenas investigated. Any rise in potential leaching intensity relative to IM stemming either from more inputs of rainfall (catenas in the sub-humid zone) or greater upslope contributing area (as in IL) resulted in reduced clay storage represented by narrower clay-rich zones. In the same way,

Table 1
Soil profile field descriptions for selected horizons from crests and most distal pedons sampled along Kruger catenas, codes from (Schoeneberger et al., 1998).

Depth	Horizon	Location (UTM) Easting	Northing	Distance from crest (m)	% gravel	Texture	Structure	Moist color	Roots
Arid zone									
DH1		316352	7453989	0					
0–2	A				10	ls	sg	7.5YR3/4	–
16–28	2Bw2				40	ls	1vfsbk	7.5YR3/4	2vf, f, 1vc
28–45	2 C				70	–	m		–
DH3		315951	7453896	320					
0–1	A				15	ls	sg	10YR3/2	1vf
1–19	Bw1				70	s	sg,m	10YR3/3	1vf,2f,1c
DM1		318626	7450293	0					
0–12	BA				70	s	sg	7.5YR2.5/2	1vf,f
29–53	C				90	s	sg	7.5YR2.5/3	1vf,f,m
53–63	CR				95	–	m		
DM6		318626	7450293	350					
0–4	A				18	ls	1vfsg	10YR3/4	1vf,f
52–76	Btk2				5	ls	2msbk,cosbk	10YR4/6	1vf
87–97	C				60	–	m		
DL1		322713	7452153	0					
0–23	BA				80	s	sg	7.5YR2.5/2	2f,vf,1m
23–45	BC				90	s	sg	7.5YR3/4	1f,m,2vf
45–55	C				100	–			
DL7		323478	7451179	970					
0–1	BAs				40	ls	1vfgr,sg	7.5YR3/3	no roots
1–11	Btk1				5	scl	1f,vfsbk	7.5YR3/3	2vf
68–95	2Bw2				0	scl	3co,coabk	7.5YR3/4	1vf
Semi-arid zone									
IH1		346001	7227674	0					
0–10	BA				30	s	1vnpl,1f,msbk,1f,mgr	10YR3/4	2vf,f
23–50	BC				80	s	sg,1fgr	7.5YR3/4	1vf,f
50–60	CR				100		M	–	–
IH5		346208	7227883	410					
0–10	BA				0	scl	sg,3f,mabk	10YR2/2	
49–83	Bt3				5	scl	2msbk,sg	5YR2.5/1	
83–93	BCR				50		M		
IM1		348286	7230808	0					
0–7	BA				5	s	1f,msbk,1fgr	10YR3/3	1vf,f
33–65	CR/BC				70	ls	sg,1fgr	10YR4/4	1f
65–75	RC				95		M	–	–
IM8		348775	7230314	700					
0–7	BA				0	s	2f,msbk,1fgr,sg	10YR2/2	1vf,f,m
7–25	Bt1				0	scl	3f,mabk,cl	10YR3/1	1vf,f,m,co
62–90	BC				0	scl	2vf,fabk,sbk,1fgr,sg	10YR4/2	–
IL1		363444	7235287	0					
1–3	A				35	s	1f,mgr,1–2tnpl	10YR3/4	2vf
3–11	BC				50	s	1vf,f,sbk	10YR3/6	1vf,f
11–30	CR				80		M		
IL10		363892	7236772	1600					
0–7	AB				0	sil	1f,msbk	10YR3/3	1vf,f
85–111	3Bt4				60	scl	2f,mabk	10YR3/3	1vf
111–120	4BC				80	sl	–	–	–
Sub-humid zone									
WH1		321217	7211736	0					
0–4	AB				0	s	1f,msbk,1fgr	10YR2/1	2vf,f
146–180	2Bw6				0	s	sg,1f,msbk	5YR4/4	1vf,f
180–212	C				5	sl	–	–	–
WH6		321655	7210984	900					
0–10	BA				0	scl	1fgr,1,2f,msbk	10YR2/1	3f,m
80–106	2Bt4				10	c	2–3m,coabk	10YR4/2	1vf
106–116	2BtC				25	c	–	–	–
WM1		323726	7211482	0					
0–10	BA				5	s	3m,coabk	10YR3/3	3vf,f,1m,vc
135–157	2Bw5				50	s	m,1vf,fsbk,sg	5YR4/4	1vf,f
157–170	3BC				72	s	1vfabk,m,sg	5YR4/4	1vf
WM11		322442	7210894	1367					
0–10	AB				5	s	1vf,f,sbk,1mgr	10YR2/2	3vf,f
95–120	2Bt2				15	scl	m	10YR3/1	1vf
120–135	3BC				70	scl	m,sg	–	–
WL1		0326823	7211630	0					
0–8	AB				0	s	0sg/1vfsbk	10YR2/2	2vff
8–17	Bw1				2	s	1vfmsbk/0sg	7.5YR3/3	3vff1c
230–245	3BC4				45	s	0ma	7.5YR5/6	–

Table 1 (*continued*)

Depth	Horizon	Location (UTM) Easting	Northing	Distance from crest (m)	% gravel	Texture	Structure	Moist color	Roots
Sub-humid zone									
WL6		0327296	7210546	1210					
0–11	BA				20	s	sg,1f,msbk,1fgr	7.5YR2.5/1	3vf,f
63–84	Bt3				30	sc	3co,vcabk	Gley 1 7/10y	1vf,f
84–120	2Bt4				15	scl	3m,coabk	Gley 1 5/10y	1vf,f

catenas that were drier than IM as a result of both lower rainfall inputs (arid zone catenas) as well as smaller contributing area (as in IH) had narrower clay-rich zones (Fig. 3).

3.2. Clay mineralogy

Kaolinite occurred in all sampled profiles while smectite was detected in about half, mostly in the arid zone (Table 4). Along arid catenas, smectite was recorded in four out of the nine B horizons evaluated, and of the four, two distally located horizons of DM had more smectite than kaolinite (Table 4). In the semi-arid zone, six of the ten B horizons had smectite, and of these, only one had more smectite than kaolinite. The rainfall-driven switch in clay mineral occurrence and abundance was most clearly apparent in the minimal occurrence of smectite in the sub-humid catenas (Table 4). Higher rainfall thus resulted in lower clay concentrations within soil profiles near the crests, narrower clay-rich zones and a greater proportion of kaolinite relative to smectite. By landscape position, kaolinite dominated the crest and near-crest positions while smectite was most abundant in the toeslopes. However, the general decline in smectite as rainfall increased reached the point where kaolinite became dominant even in the toeslope soils of the sub-humid catenas (Table 4).

3.3. Potential cation exchange capacity

DH had CECs below 7 $cmol_{(+)} kg^{-1}$ from the crest to the footslope, and DM had similarly low CECs in the clay-poor zone, from 8.7 at the crest to 12 $cmol_{(+)} kg^{-1}$ in DM3, CECs then increased in the clay-rich zone to a 21 $cmol_{(+)} kg^{-1}$ peak in DM4 (Fig. 4 and Table 2). DL displayed CECs similar to DM's, 11 to 14 $cmol_{(+)} kg^{-1}$ from the crest to DL6 while DL7 had the peak CEC of 25 $cmol_{(+)} kg^{-1}$. CECs in the semi-arid zone were in the same general range as in the arid zone, 2.1 to 28 $cmol_{(+)} kg^{-1}$ and 3 to 25 $cmol_{(+)} kg^{-1}$, respectively. IH had low CECs in the clay-poor zone (8.7 $cmol_{(+)} kg^{-1}$ and below) and higher CECs in the two soils of the clay-rich zone, the peak CEC was 28 $cmol_{(+)} kg^{-1}$ in the last soil of the sequence. IM had a more extensive zone of relatively higher CEC enveloping the soils between IM5 (with a CEC of 17 $cmol_{(+)} kg^{-1}$) and the terminal profile, IM8 (28 $cmol_{(+)} kg^{-1}$), the intervening soils, IM6 to IM7 had CECs of 26 and 28 $cmol_{(+)} kg^{-1}$ respectively. Similarly, IL1 to IL5 had CECs in the range 2.1 to 3.8 $cmol_{(+)} kg^{-1}$ while the downslope soils from IL6 to IL10 ranged between 12 and 25 $cmol_{(+)} kg^{-1}$. The most noteworthy CEC distinction of the sub-humid soils from both drier zones was a steep decline in the CEC of clay-poor soils, but ranges overlapped generally with those in the arid and semi-arid zones (2.2 to 39 $cmol_{(+)} kg^{-1}$). WH had CECs between 3.3 and 6.7 $cmol_{(+)} kg^{-1}$ between the crest and WH5, while WH6 had the highest CEC recorded in the whole study (39 $cmol_{(+)} kg^{-1}$). WM had a peak CEC of just 11 $cmol_{(+)} kg^{-1}$ in WM10 while the rest of its soils had CECs below 10 $cmol_{(+)} kg^{-1}$. WL had relatively high CECs even in the near crest positions, only one soil (IL2, 4.7 $cmol_{(+)} kg^{-1}$) had a CEC below 10 $cmol_{(+)} kg^{-1}$, while all the other soils had CECs between 11 (at the crest) and 22 $cmol_{(+)} kg^{-1}$ in IL6, the most distal soil sampled.

3.4. Base cation concentrations

The concentrations of base cations, Na, K, Ca and Mg were between <1 and 23 $cmol_{(+)} kg^{-1}$ in the arid catenas, <1 to 19 $cmol_{(+)} kg^{-1}$ in the semi-arid zone and <1 to 8 $cmol_{(+)} kg^{-1}$ in the sub-humid zone (Fig. 5 and Table 2). In the arid zone, DH sodium ranged from <1 at the crest to 1.1 $cmol_{(+)} kg^{-1}$ in DH3. DM generally displayed an increase in Na with increasing distance from the crest to a maximum Na content of 3.7 $cmol_{(+)} kg^{-1}$ in DM6, the terminal soil. On DL, there was no marked increase in Na down the transect and the range in concentration fell between <1 in five soils and 1.6 $cmol_{(+)} kg^{-1}$ in DL6 (Fig. 5). In IH, concentrations of Na fell at or below 1 $cmol_{(+)} kg^{-1}$. Downstream in IM, Na reached its peak concentration among all soils sampled in the study, 13 $cmol_{(+)} kg^{-1}$ in IM8, concentrations elsewhere on this hillslopes were between <1 and 2.7 $cmol_{(+)} kg^{-1}$. In IL, Na concentrations were all below 1 $cmol_{(+)} kg^{-1}$. The sub-humid catenas' Na concentrations consistently increased towards the toe-slopes. In WH, sodium content rose from lows under 1 $cmol_{(+)} kg^{-1}$ from the crest to WH5 to the peak 1.1 $cmol_{(+)} kg^{-1}$ in WH6. Likewise, Na on WM reached a peak of 3.6 in WM10, while the zone from the crest to WM9 had magnitudes below 1 $cmol_{(+)} kg^{-1}$. WL was not as highly depleted in Na as WM, concentrations there were between <1 and 6.6 $cmol_{(+)} kg^{-1}$.

Potassium concentrations in DH were all below 1 $cmol_{(+)} kg^{-1}$. On DM, K concentrations increased downslope to as high as 9.6 $cmol_{(+)} kg^{-1}$ in DM6 while soils upslope of the peak generally had less than 1 $cmol_{(+)} kg^{-1}$ except 1.5 $cmol_{(+)} kg^{-1}$ in DM4. Similarly, DL soils only reached concentrations above 1 $cmol_{(+)} kg^{-1}$ in the last two soils sampled, which had 1.5 and 23 $cmol_{(+)} kg^{-1}$ K respectively, the highest K observed. Rising rainfall generally resulted in less K across the catenas, the range in the semi-arid zone was <1 to 3.9 $cmol_{(+)} kg^{-1}$. IH had levels of K below 1 $cmol_{(+)} kg^{-1}$ in all observations. In IM, K was again less than 1 $cmol_{(+)} kg^{-1}$ throughout while in IL concentrations were between <1 and 3.9 $cmol_{(+)} kg^{-1}$. The sub-humid soils had even less K in them with none reaching even 1 $cmol_{(+)} kg^{-1}$.

The divalent base cations generally occurred in greater abundance across the catenas than Na and K. In DH, magnesium rose from <1 $cmol_{(+)} kg^{-1}$ at the crest to 1 $cmol_{(+)} kg^{-1}$ at the footslope, while peak Mg on DM was 6.8 in DM3 and on DL 6.6 $cmol_{(+)} kg^{-1}$ in DL6. Higher rainfall in the semi-arid zone hardly affected the Mg content, which was between <1 and 7.5 $cmol_{(+)} kg^{-1}$. IH displayed increased Mg content downslope from <1 in IH2 to 4.9 $cmol_{(+)} kg^{-1}$ in IH4. IL had peak Mg of 7.5 $cmol_{(+)} kg^{-1}$ in the second last soil sampled with generally increasing Mg downslope from the crest to DL10. Many more soils in the sub-humid zone had less than 1 $cmol_{(+)} kg^{-1}$ Mg compared to catenas in the drier climates. Peak Mg in the whole study occurred in the sub-humid zone's WH6 which reached 8 $cmol_{(+)} kg^{-1}$ Mg, the zone on the upslope side of WH6, representing 99% of the catena, had below 1 $cmol_{(+)} kg^{-1}$ Mg except in WH4 which was 2.2 $cmol_{(+)} kg^{-1}$. WL had increasing Mg content downslope with the

Table 2
Selected chemical and physical properties of soil horizons from crests and most distal profiles sampled on catenas in Kruger.

Depth (cm)	Horizon	Clay%	xK (cmol(+) kg^{-1})	xMg	xCa	xNa	CEC	BS (%)	Fizz	pH	EC (mS cm^{-1})
Arid zone											
DH1											
0–2	A	8	0.34	0.60	0.98	0.60	2.69	94	ne	5.3	<0.1
16–28	2Bw2	11	0.14	0.56	0.49	0.55	2.48	70	ne	4.8	<0.1
28–45	2 C	–	–	–	–	–	–	–			
DH3											
0–1	A	11	0.42	1.06	2.68	1.05	5.24	99	ne	5.8	nd
1–19	Bw1	8	0.28	1.10	0.94	1.09	3.00	114	ne	5.4	nd
DM1											
0–12	BA	5	1.08	2.19	4.85	0.31	11.19	75	ne	6.3	<0.1
29–53	C	5	1.02	2.08	2.23	0.40	7.02	82	ne	6.4	<0.1
53–63	CR	–	–	–	–	–	–	–			
DM6											
0–4	A	2	0.51	1.40	4.64	1.05	12.00	63	ne	7.3	<0.1
52–76	Btk2	10	13.20	2.18	19.81	0.56	11.51	311	ve	7.7	2.7
87–97	C	–	–	–	–	–	–	–	st		
DL1											
0–23	BA	6	0.36	1.20	5.04	0.98	10.40	73	ne	6.1	<0.1
23–45	BC	5	0.30	1.06	3.53	0.82	11.63	49	ne	5.9	<0.1
45–55	C	–	–	–	–	–	–	–			
DL7											
0–1	BAs	12	9.77	1.94	4.22	0.53	18.21	90	ne	6.7	1.8
1–11	Btk1	22	22.63	5.85	18.26	0.78	25.99	183	st	7.7	9.4
68–95	2Bw2	21	21.01	3.07	3.56	0.91	24.52	116	ne	7.4	6.3
Semi-arid zone											
IH1											
0–10	BA	3	0.60	1.28	1.89	0.32	6.67	61	ne	5.8	<0.1
23–50	BC	7	0.62	2.07	1.61	0.34	10.00	46	ne	4.8	<0.1
50–60	CR										
IH5											
0–10	BA	26	1.03	3.72	8.37	0.72	22.22	62	ne	6.2	<0.1
49–83	Bt3	35	0.55	3.39	14.54	0.35	30.04	63	ne	7.3	0.2
83–93	BCR										
IM1											
0–7	BA	7	0.92	1.55	1.63	0.57	6.23	75	ne	6.1	<0.1
33–65	CR/BC	10	0.42	2.07	1.23	0.59	7.98	54	ne	5.2	<0.1
65–75	RC										
IM8											
0–7	BA	2	0.83	1.52	2.94	1.12	9.40	68	ve	6.7	0.1
7–25	Bt1	25	0.80	6.55	3.78	9.84	26.94	78	sl	8.6	1.5
62–90	BC	30	0.70	7.26	13.21	15.59	28.57	128	sl	9.1	2.9
IL1											
1–3	A	2	0.48	0.85	1.17	0.49	6.79	44	ne	5.6	<0.1
3–11	BC	3	0.24	0.84	0.77	0.56	5.32	45	ne	5.2	<0.1
11–30	CR										
IL10											
0–7	AB	10	1.0	5.1	9.30	0.39	18.49	85	ne	7.0	0.2
85–111	3Bt4	27	2.4	7.1	21.61	0.61	28.13	112	ne	8.3	0.5
111–120	4BC	17	2.6	6.8	19.24	0.43	24.56	118	ne	8.6	0.4
Sub-humid zone											
WH1											
0–4	AB	2	0.56	2.55	3.62	0.53	7.98	91	ne	6.2	<0.1
146–180	2Bw6	6	0.23	1.59	0.88	0.63	4.29	78	ne	5.5	<0.1
180–212	C	17	0.24	2.26	1.30	0.62	5.63	79	ne	6.0	<0.1
WH6											
0–10	BA	21	0.50	2.76	2.60	0.62	19.01	34	ne	4.8	0.1
50–80	Bt3	88	0.39	10.07	7.73	1.22	43.65	44	ne	6.2	0.0
106–116	2BtC	40	0.26	6.07	4.74	1.01	25.99	47	ne	6.6	<0.1
WM1											
0–10	BA	5	0.12	0.45	1.41	0.02	5.61	36	ne	5.8	0.1
135–157	2Bw5	8	0.12	0.29	0.55	0.06	4.88	21	ne	5.7	0.1
157–170	3BC	10	0.17	0.47	0.82	0.07	5.25	29	ne	5.9	<0.1
WM11											
0–10	AB	6	0.24	1.01	1.88	0.06	5.90	54	ne	5.5	0.1
95–120	2Bt2	27	0.19	5.50	7.32	0.74	11.71	117	ne	6.7	0.1
120–135	3BC	24	0.23	5.37	7.01	0.77	13.60	98	ne	6.4	0.1
WL1											
0–8	AB	3	0.07	0.31	1.14	0.12	32.82	5	ne	6.4	0.11
8–17	Bw1	3	0.06	0.23	1.06	0.11	8.01	18	ne	6.0	0.01
230–245	3BC4	8	0.11	0.62	1.85	0.15	14.42	18	ne	6.1	0.00
WL6											
0–11	BA	4	0.48	2.22	2.57	0.52	10.79	53	ne	5.6	<0.1
63–84	Bt3	35	0.41	7.27	5.77	4.39	21.19	84	ne	8.5	0.7
84–120	2Bt4	30	0.36	8.34	5.39	5.76	26.90	73	ne	8.4	0.9

Table 3
Soil classification, distance of study pedons relative to reference crests, clay amount and clay contrast indices at the profile (within-profile) and catena (between-profile) scales.

Climate zone catena/pedon	Soil classification	Distance from crest (m)	Clay %	Within-profile clay contrast index	Between-profile clay contrast index
DH1	Haplocambid	15	11	0.22	0.19
DH2	Haplocambid	130	14	0.37	
DH3	Haplocambid	320	9	0.00	
DM1	Haplocambid	15	5	0.00	0.81
DM2	Haplocambid	180	6	0.29	
DM3	Paleargid	220	24	0.58	
DM4	Paleargid	275	19	0.80	
DM5	Paleargid	295	15	0.65	
DM6	Natragid	350	11	0.88	
DL1	Haplocambid	15	6	0.00	0.77
DL2	Haplocambid	150	5	0.34	
DL3	Haplocambid	270	8	0.50	
DL4	Haplocambid	380	4	0.58	
DL5	Paleargid	500	8	0.81	
DL6	Natragid	850	17	0.57	
DL7	Paleargid	970	24	0.55	
IH1	Ustorthent	15	7	0.63	0.77
IH2	Dystrustept	170	6	0.38	
IH3	Ustorthent	270	5	0.75	
IH4	Kanhaplustalf	340	25	0.83	
IH5	Kanhaplustalf	410	32	0.25	
IM1	Ustorthent	15	9	0.25	0.71
IM3	Dystrustept	225	1	0.50	
IM4	Dystrustept	330	7	0.33	
IM5	Natrustalf	425	20	0.66	
IM6	Natrustalf	500	30	0.71	
IM7	Kanhaplustalf	610	21	0.20	
IM8	Natrustalf	700	28	0.93	
IL1	Ustorthent	15	3	0.33	0.87
IL2	Dystrustept	400	5	0.31	
IL3	Dystrustept	755	4	0.00	
IL4	Dystrustept	895	3	0.07	
IL5	Ustorthent	977	3	0.14	
IL6	Dystrustept	1123	17	0.70	
IL7	Dystrustept	1275	26	0.54	
IL8	Kanhaplustalf	1385	17	0.50	
IL9	Kanhaplustalf	1550	21	0.81	
IL10	Kanhaplustalf	1600	23	0.64	
WH1	Dystrustept	15	13	0.86	0.80
WH2	Dystrustept	300	6	0.43	
WH3	Dystrustept	544	7	0.28	
WH4	Dystrustept	820	4	0.75	
WH5	Dystrustept	860	11	0.20	
WH6	Kanhaplustalf	900	65	0.76	
WM1	Dystrustept	15	8	0.50	0.76
WM2	Dystrustept	20	10	0.49	
WM3	Dystrustept	225	10	0.73	
WM4	Dystrustept	397	8	0.77	
WM5	Dystrustept	513	4	0.14	
WM6	Dystrustept	640	4	0.62	
WM7	Dystrustept	777	5	0.66	
WM8	Dystrustept	1048	6	0.56	
WM9	Kanhaplustalf	1133	35	0.79	
WM10	Kanhaplustalf	1223	26	0.56	
WM11	Kanhaplustalf	1376	17	0.79	
WL1	Dystrustept	15	9	0.83	0.72
WL2	Dystrustept	546	4	0.57	
WL3	Dystrustept	1000	9	0.95	
WL4	Kanhaplustalf	1060	20	0.83	
WL5	Ustorthent	1185	17	0.94	
WL6	Kanhaplustalf	1210	30	0.90	

peak in the last soil, WL6 at 6.6 $cmol_{(+)} kg^{-1}$. Calcium was <1 to 2 $cmol_{(+)} kg^{-1}$ in DH, 1.2 to 18 $cmol_{(+)} kg^{-1}$ in DM and <1 and 14 $cmol_{(+)} kg^{-1}$ in DL. The peaks in Ca concentration were in DH2, DM4 and DL6 respectively across the arid catenas. In IH the pattern was erratic but the peak occurred in the IH5 (13 $cmol_{(+)} kg^{-1}$) and minimum Ca content was in IH3 (<1 $cmol_{(+)} kg^{-1}$). In IM, peak Ca was in IM6 at 18 $cmol_{(+)} kg^{-1}$ while the lowest concentration was <1 in IM3. WL had increasing Ca amount from the crest to footslope, from lows under 1 $cmol_{(+)} kg^{-1}$ between the crest and IL5, to highs in the range 2.5 (in IL6) to 19 $cmol_{(+)} kg^{-1}$ (in IL9) in the remaining soils. As with the other base cations, magnitudes of Ca concentration in the sub-humid soils were lower than in the arid to semi-arid zone. Calcium concentrations on WH were 1 $cmol_{(+)} kg^{-1}$ and less from the crest to WH5 while WH6 had 6.2 $cmol_{(+)} kg^{-1}$ Ca. WM exhibited a similarly increasing trend in Ca concentration downslope, <1 to 4.1 $cmol_{(+)} kg^{-1}$. Finally, WL Ca was in the range <1 to 5.2 $cmol_{(+)} kg^{-1}$.

3.5. Base saturation

Base saturations across the catenas ranged between 12% in WM5 to 100% in DH3 (Fig. 4 and Table 2). The arid zone had the highest base saturations, the semi-arid zone had the next highest while the sub-humid soils displayed the lowest. In DH, all profiles had base saturations in excess of 70%. This was also generally true for DM whose two most distal soils had base saturations above 90%. DL had base saturations in the range 37% (in DL4) to 100% in DL6 and 90% in DL7. The semi-arid soils had base saturations spanning 23% (IL4) and 93% (IL9). In IH, base saturation ranged between 50 (the crest) and 88% (IH4), on IM, between 53 (the crest) and 93% (IL8, the last soil sampled), while in DL between 16 (the crest) and 93% (IL9). Finally, in the sub-humid zone, as previously stated, there was a sharp decline in base saturations as evident in most crests and near-crest locations. WH ranged from 15.2 (WH3) to 79% (WH4), WM was between 15.1 and 87% while on WL the range was 18 to 70%.

4. Discussion

Clay mineralogy and clay content varied systematically within and between soil profiles following consistent patterns under the combined controls of rainfall and catena position in Kruger National Park. Along each catena from the crest to the toe, depth and clay content increased, and in dry catenas, there was more smectite downslope while in the wettest none was detected. Thus increased rainfall generally resulted in deeper soils, less clay broadly and less smectite in particular. The fluctuating soil morphology as a function of landscape context went in concert with changing soil chemical properties. Accordingly, CEC and base saturation across the hillslopes were determined by rainfall and catena position. Under dry conditions, exchange sites were generally more saturated and the degree of saturation increased downslope. In the wettest soils, the downslope increasing saturation of exchange sites persisted but from a low base to even lower magnitudes. The morphological and chemical changes in the soils modulate the function of catenas as media for biota and as integral elements of the savanna landscape.

The clay-rich zones along each catena function as hydrological boundaries separating zones of sub-surface flow in porous clay-poor soils from zones dominated by surface flow induced by restricted drainage in clay-rich profiles. The changing hydrological conditions create an approximately 1–10 m seepzone immediately above the first clay-rich profile from the crest. The seepzone created on each catena, by the diverted water separates different biogeochemical process domains on either side. Soils at the seepzone are periodically inundated and are under reducing conditions during wet periods. Soils above the seepzone are the source zone of soil constituents including clays while soils below are recipients of upslope derived soil material. It follows that since the extent of process zones on the

Note to Table 2:
x represents the exchangeable form of the cation. Fizz means effervescence upon addition of dilute HCl onto the soil matrix to test for carbonate presence and qualitative amount, ne is "no bubbles formed", vs is "few bubbles form", sl is "numerous bubbles form", st is "bubbles form a low foam" and ve is "bubbles form a thick foam" (Schoeneberger et al., 1998).

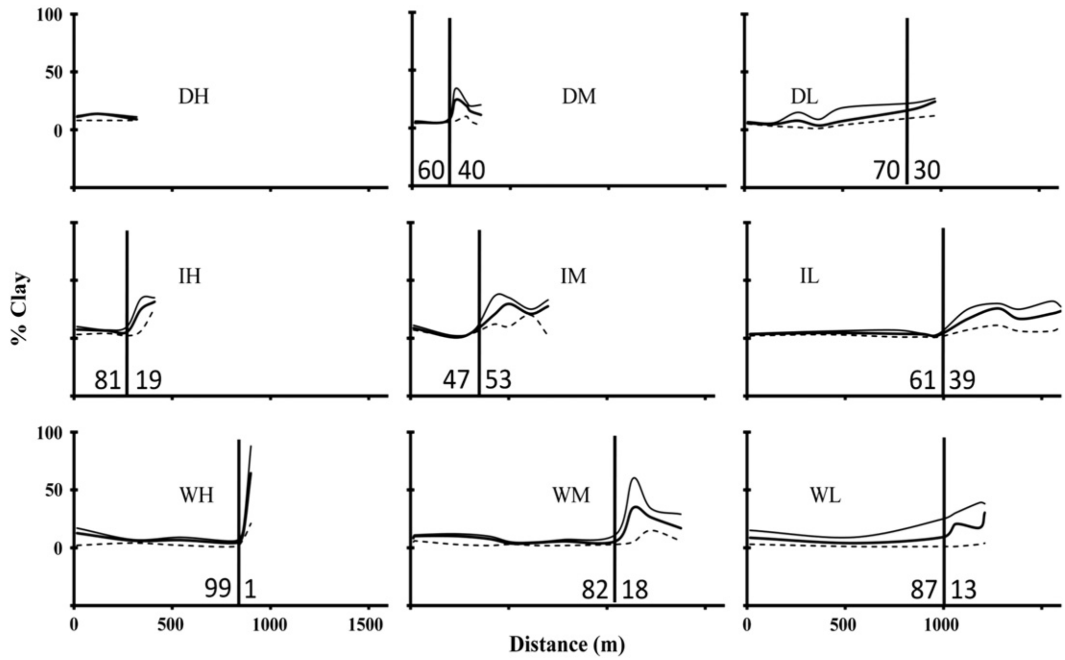

Fig. 3. Clay concentrations in soil profiles across catena (minimum, dotted) (depth-weighted average, bold solid line) (maximum, solid line), vertical lines designate the boundary between clay-poor (to the left) and clay-rich soils (to the right) with the percent hillslope occupied by each zone.

catenas is altered by climate and topography, the extent and importance of particular biogeochemical zones also change with state factors. Therefore, wet catenas with their broad seepzones can be regarded as gigantic reducing media. Under semi-arid rainfall the seepzone emerges at 80% of the hillslope's extent from the crest and thus the sphere of reduced soils is only a sliver on the catena. Under the driest conditions the seepzone is even narrower or non-existent as in DH. These variations in soil morphology and biogeochemistry are the origins of landscape heterogeneity.

By exploring the imprint of other soil forming factors, the value of viewing landscapes as catenas can be appreciated even more. For example, the climosequence of catenas studied here can be extended

Table 4
Clay fraction smectite, kaolinite and quartz abundances in selected horizons analyzed by X-ray diffraction. Abundances represent peak intensity ratios with 0 = not detected, 1 = <20%, 2 = 20–40%, 3 = 40–60%, 4 = 60–80% and 5 = 80–100%. Also shown are clay %, soil CEC, and organic C for the reference horizons. Position on catena is given as a proportion of hillslope in pedon location where 0% is the crest and 100% the entire catena.

Site	Position on catena (%)	Depth	Smectite	Kaolinite	Quartz	Clay %	CEC (cmol(+) kg^{-1})	Organic C (%)
DH1	5	13–22	1	1	1	15	5	0.4
DH2	39	14–23	0	1	1	14	3	0.4
DH3	97	0–1	0	1	1	11	5	0.7
DM1	4	12–29	0	1	1	4	9	0.5
DM4	75	51–63	5	1	2	18	26	
DM6	96	76–87	5	1	1	20	22	
DL1	1	23–45	1	2	2	5	12	0.8
DL3	22	2–19	0	1	1	3	12	
DL7	79	11–40	0	1	1	25	27	
IH1	4	0–10	1	1	1	4	7	0.6
IH3	64	26–40	1	1	2	5	4	
IH5	98	31–49	3	1	2	33	30	
IM5	47	25–62	0	1	1	34	30	
IM7	68	25–46	1	1	1	30	34	
IL1	1	3–11	0	1	2	4	5	0.3
IL6	61	1–24	0	1	1	5	6	
IL7	69	1–16	0	1	1	11	15	
IL9	84	35–57	1	1	2	25	25	
IL10	86	34–60	3	3	3	28	24	
WH4	90	24–47	0	2	2	5	4	
WH6	99	29–50	0	5	5	58	44	
WL1	1	93–115	0	3	3	10	12	0.1
WL2	45	71–94	0	1	5	1	4	
WL3	82	45–60	2	4	3	5	6	
WL4	87	0–9	0	1	3	5	9	
WL5	97	0–11	1	1	3	4	11	
WL6	99	40–63	2	3	2	30	22	
D-Basalt	~5	B-horizon	≫5	0	0			
D-Gabbro	~5	B-horizon	≫5	1	1			

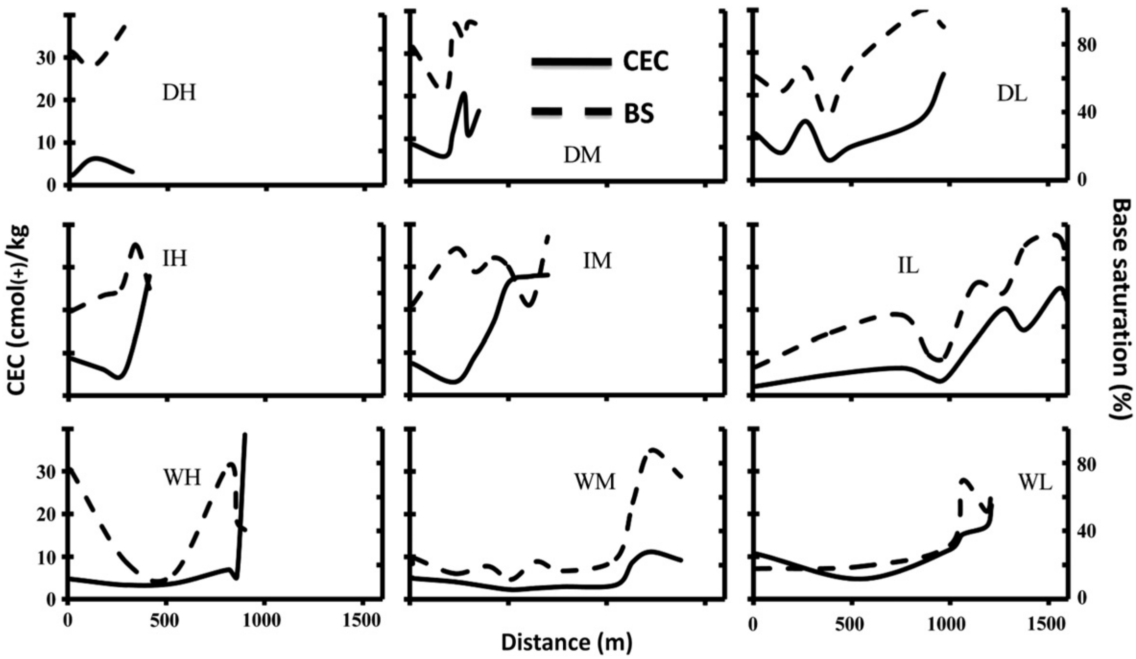

Fig. 4. Depth-weighted average CEC and base saturation across climate and slope-length classes in Kruger.

into different geological formations such as the gabbro adjacent to the Kruger granites. What distinguishes gabbro from granite is its more mafic geochemistry which yields clay-rich soils all across the Kruger climate gradient (Venter, 1990). Hence the CEC and base saturation of gabbro catenas can be expected to be much higher than that of corresponding granitic catenas while the clay mineralogy of gabbroic soil is predominantly smectitic due to lack of free drainage (Table 4). Investigating soil forming factor control on catenas will benefit our understanding of the geochemical functioning of catena soils and how they condition landscape morphology, evolution, biogeochemistry and heterogeneity.

The implication of pedogenic diversity on biogeochemistry can be illustrated by the distribution of nutrients in the ecosystems that these catenas nourish. Much work in southern Africa has shown that catenas have clear relationships with soil nutrient content (Scholes and Walker, 1993) and plant distribution (Dye and Walker, 1980). The classical view is that fine-leaf nutrient rich patches occur in clay-rich toeslopes while broad-leaf nutrient poor patches occur in sandy soils

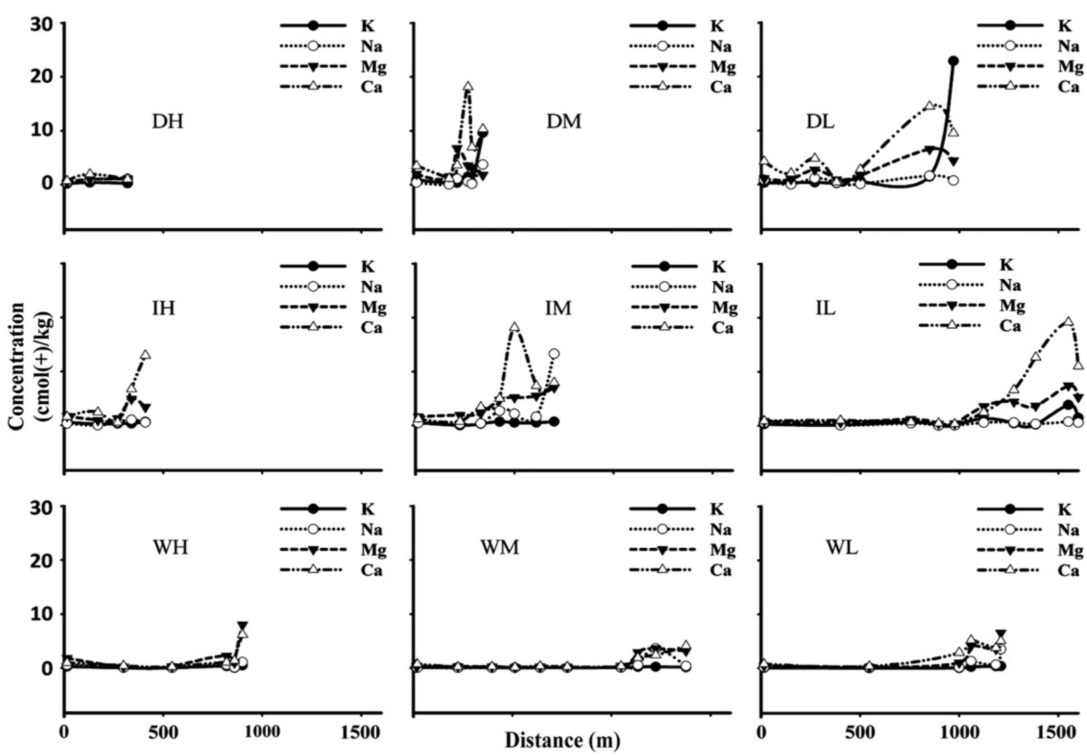

Fig. 5. Depth-weighted average concentrations of base cations across catenas in Kruger.

on crests and nearby. Nutrient-rich patches in our studied catenas would occupy the clay-rich zones in Fig. 3 as corroborated by the elevated concentrations of base cations therein. Significantly, the extent of nutrient-rich zones is configured by the morphology and chemistry of soils on the catenas, with some catenas like DH having no nutrient-rich patches at all due to soils with limited differentiation. It could also be envisaged that a catena wetter than WH would also lack nutrient-rich patches as a result of complete removal of the narrow (1% of the hillslope) clay-rich band. The catena concept can be applied in any landscape to explain the occurrence of distinct biogeochemical and biological domains in physiographically defined landscape segments. Levick et al. (2010) used remote imaging to show that the distribution of termite mounds and woody vegetation follows systematic patterns controlled by catena soil properties like clay content. This reinforces the view that catenas are the physical template of savanna heterogeneity (Venter et al., 2003) and regulate the interactions between biota and their physical environment. In this study we have shown how these controls originate and how they vary spatially along climo-topographic gradients in Kruger National Park.

It is interesting that most studies on African catenas were conducted in the 400 to 800 mm rainfall range (see Paton et al., 1995 for an extensive review). It appears that this rainfall amount is ideal for inducing peak heterogeneity in catena soil properties, assuming that other soil forming factors stay uniform. Outside these rainfall limits, as illustrated by catenas in the three rainfall zones presented here, distinct catena elements either do not emerge due to limited rainfall or they are homogenized by excessive rainfall. The fact that granite has been the parent material upon which African catenas become well-expressed also suggests that this substrate is ideal for the formation of a classic catena sequence. As illustrated here with gabbro, a more mafic parent material limits soil differentiation, and it can also be hypothesized that a parent material more felsic than granite such as rhyolite would have its own peculiar mode of catena development.

The catenas of Kruger National Park studied here constitute an ideal model of soil development mediated by climate, topography and landscape position in the granitic region of southern Africa, which extends into Zimbabwe (Watson, 1964), East Africa where catenas were originally described (Milne, 1935). Results from this study will apply equally in all these and similar regions characterized by savanna vegetation experiencing rainfall less than 1000 mm per year and sufficiently stable for soil development to occur uninterrupted by geotectonic forces.

Acknowledgments

This project was funded by the Andrew W. Mellon Foundation. Thanks to the South African National Parks for granting permission to work in the Kruger National Park. We thank Frank Setaro, Wilsoni Dinda, Samuel Nkuna and Million Cossa, Val Bullard, Kevin Bratton, Nathalie Boes, Dasha Perkins, Caroline Guebels, Katie Lindeburg, Angela Gaylard, Freek Venter and Wendy Midgely for assistance in the laboratory, office and field. We would also like to greatly thank the editor and two anonymous reviewers for their patience in substantially improving the manuscript.

References

Barton, J.M., Bristow, J.W., Venter, F.J., 1986. A summary of the Precambrian granitoid rocks of the Kruger National Park. Koedoe 29, 39–44.
Birkeland, P.W., 1999. Soils and Geomorphology. Oxford University Press, Oxford.
Carter, M.R., 1993. Soil Sampling and Methods of Analysis. Lewis Publishers, Boca Raton.
Chadwick, O.A., Gavenda, R.T., Kelly, E.F., Ziegler, K., Olson, C.G., Elliott, W.C., Hendricks, D.M., 2003. The impact of climate on the biogeochemical functioning of volcanic soils. Chemical Geology 202 (3–4), 195–223.
Chadwick, O.A., Graham, R.C., 1999. Pedogenic processes. In: Sumner, M.E. (Ed.), Handbook of Soil Science. CRC Press, New York.
Conacher, A.J., Dalrymple, J.B., 1977. 9 unit land-surface model: approach to pedogeomorphic research. Geoderma 18 (1–2), 1–154.
Dye, P.J., Walker, B.H., 1980. Vegetation–environment relations on sodic soils of Zimbabwe, Rhodesia. Journal of Ecology 68, 589–606.
Fey, M., 2010. Soils of South Africa. Cape Town, Cambridge.
Gertenbach, W.P.D., 1983. Landscapes of the Kruger National Park. Koedoe 26, 9–121.
Huggett, R.J., 1975. Soil landscape systems: a model of soil genesis. Geoderma 13 (1), 1–22.
Khomo, L., 2008. Weathering and soil properties on old granitic catenas along climo-topographic gradients in Kruger National Park. PhD Thesis, University of the Witwatersrand, Johannesburg.
Levick, S.R., Asner, G.P., Chadwick, O.A., Khomo, L.M., Rogers, K.H., Hartshorn, A.S., Kennedy-Bowdoin, T., Knapp, D.E., 2010. Regional insight into savanna hydrogeomorphology from termite mounds. Nature communications 1 article no. 65.
Liao, N., 2001. Determination of ammonia by flow injection analysis. QuickChem Method 10-107-06-1-J. Lachat Instruments, Loveland, Colorado.
Milne, G., 1935. Some suggested units of classification and mapping, particularly for East African soils. Soil Research 4, 183–198.
Nye, P.H., 1954. Some soil forming processes in the humid tropics I: a field study of a catena in the West African forest. Journal of Soil Science 5, 7–21.
Paton, T.R., Humphreys, G.S., Mitchell, P.B., 1995. Soils: a New Global View. Yale University Press, New Haven.
Radwanski, S.A., Ollier, C.D., 1959. A study of an East African catena. Journal of Soil Science 10, 149–168.
Schoeneberger, P.J., Wysocki, D.A., Benham, E.C., Broderson, W.D., 1998. Field Book for Describing and Sampling Soils. National Soil Survey Center Natural Resources Conservation Service U.S. Dept. of Agriculture, Lincoln, Nebraska.
Scholes, R.J., Bond, W.J., Eckhardt, H.C., 2003. Vegetation dynamics in the Kruger ecosystem. In: du Toit, J.T., Rogers, K.H., Biggs, H.C. (Eds.), Ecology and Management of Savanna Heterogeneity. Island press, Corvelo.
Scholes, R.J., Walker, B.H., 1993. An African Savanna: a Synthesis of the Nylsvley Study. Cambridge University Press, Cambridge.
Soil Survey Staff, 1996. Soil survey laboratory methods manual. Soil Survey Investigation Report No. 42 Version 3.0. National Soil Survey Centre, Lincoln, NE.
Sommer, M., Halm, D., Weller, U., Zarei, M., Stahr, K., 2000. Lateral podzolization in a granite landscape. Soil Science Society of America Journal 64 (6), 2069-2069.
Sommer, M., Schlichting, E., 1997. Archetypes of catenas in respect to matter: a concept for structuring and grouping catenas. Geoderma 76 (1–2), 1–33.
USDA-NRCS, 1996. Keys to Soil Taxonomy. United States Department of Agriculture, Lincoln, NE.
Venter, F.J., 1990. A classification of land for management planning in the Kruger National Park. PhD Thesis, University of South Africa.
Venter, F.J., Scholes, R.J., Eckhardt, H.C., 2003. The abiotic template and its associated vegetation pattern. In: du Toit, J.T., Rogers, K.H., Biggs, H. (Eds.), The Kruger Experience: Ecology and Management of Savanna Heterogeneity. Island Press, Washington, DC, pp. 83–129.
Watson, J.P., 1964. A soil catena on granite in Southern Rhodesia I: field observations. Journal of Soil Science 15 (2), 239–257.
Young, A., 1976. Tropical soils and soil survey. Cambridge Geographical Studies 9. Cambridge University Press, Cambridge.